ELSEVIER

Engineering Analysis with Boundary Elements 25 (2001) 115–128

ENGINEERING ANALYSIS with BOUNDARY ELEMENTS

www.elsevier.com/locate/enganabound

A comparison of boundary element method formulations for steady state anisotropic heat conduction problems

N.S. Mera, L. Elliott, D.B. Ingham*, D. Lesnic

Department of Applied Mathematics, University of Leeds, Leeds LS2 9JT, UK

Received 20 March 2000; revised 20 July 2000; accepted 13 September 2000

Abstract

In this paper the boundary element method (BEM) is numerically implemented in order to solve steady state anisotropic heat conduction problems. Various types of elements, namely, constant elements, continuous and discontinuous linear elements and continuous and discontinuous quadratic elements are used. The performances of these various BEM formulations are compared for both the direct well-posed Dirichlet problem and the inverse ill-posed Cauchy problem, revealing several features of the BEM. Furthermore, previously undetermined analytical solutions for the integrals associated with linear and quadratic elements are presented.

Keywords: BEM; Anisotropic heat conduction

1. Introduction

There are many natural and man-made materials in which the thermal conductivity varies with direction. For example, crystals, wood, sedimentary rocks, metals that have undergone heavy cold pressing, laminated sheets, cables, heat shielding materials for space vehicles, fibre reinforced structures, and many others are anisotropic materials. In wood, for example, the thermal conductivity is different along the grain, across the grain and circumferentially. In laminated sheets the thermal conductivity is not the same along and across the laminations. Therefore, heat conduction in anisotropic materials has numerous important applications in various branches of science and engineering. Following the rapid increase of their industrial use, the understanding of heat conduction in this type of material is of great importance. However, only a limited number of works is available on the subject.

It is the purpose of this paper to numerically implement the boundary element method (BEM) in order to solve steady state anisotropic heat conduction problems. Various types of elements, namely constant, continuous and discontinuous linear elements and continuous and discontinuous quadratic elements are investigated. Furthermore, previously undetermined analytical solutions for the integrals associated with linear and quadratic elements are presented. The use of these analytical expressions instead of the previously employed quadrature formulae, see Chang et al. [3], not only reduces the programming complexity but also results in substantial reductions in computational time.

The convergence and accuracy of the BEM using various types of boundary elements are investigated and compared for both a direct well-posed problem and an inverse ill-posed problem, revealing several features of the BEM.

2. Mathematical formulation

Consider an anisotropic medium in an open bounded domain $\Omega \subset \mathbb{R}^2$ and assume that Ω is bounded by a surface Γ, which may consist of several segments, each being sufficiently smooth in the sense of Liapunov, see Jawson and Symm [6]. In this study we refer to steady heat conduction applications and therefore the function T, which denotes the temperature distribution in Ω, satisfies the equation

$$LT(\bar{x}) = k_{11}\frac{\partial^2 T}{\partial x^2} + 2k_{12}\frac{\partial^2 T}{\partial x \partial y} + k_{22}\frac{\partial^2 T}{\partial y^2} = 0, \quad \bar{x} \in \Omega \subset \mathbb{R}^2 \tag{1}$$

where we assume that heat generation is absent and the physical and thermal properties of the medium are constant, thus the coefficients k_{ij} are independent of both the space

* Corresponding author. Tel.: +44-113-233-5113; fax: +44-113-242-9925.

E-mail address: amt6dbi@amsta.leeds.ac.uk (D.B. Ingham).

0955-7997/01/$ - see front matter
PII: S0955-7997(00)00050-3

and time variables. The thermal conductivity tensor is assumed to be symmetric and positive-definite so that Eq. (1) is elliptical.

In order to illustrate and compare the convergence and the accuracy of various BEM formulations we consider two problems associated with Eq. (1), which are distinct with respect to the imposition of boundary conditions on the boundary $\partial\Omega = \Gamma = \Gamma_0 \cup \Gamma_1$, where $\Gamma_0, \Gamma_1 \neq \varnothing$ and do not intersect each other.

Example 1. First we consider the direct, well-posed interior Dirichlet problem, which consists of the solution of the steady state heat conduction equation subject to the specification of the temperature over the whole boundary, i.e. the problem to be solved is

$$\begin{cases} LT(\bar{x}) = k_{11}\dfrac{\partial^2 T}{\partial x^2} + 2k_{12}\dfrac{\partial^2 T}{\partial x \partial y} + k_{22}\dfrac{\partial^2 T}{\partial y^2} = 0 & \bar{x} \in \Omega \\ T(\bar{x}) = f(\bar{x}) & \bar{x} \in \Gamma \end{cases} \tag{2}$$

where f is a prescribed function.

Example 2. In the direct problem many experimental impediments may arise in measuring or in enforcing the boundary conditions. There are many practical applications, which arise in engineering where a part of the boundary is not accessible for temperature or heat flux measurements. For example, the temperature or the heat flux measurement may be seriously affected by the presence of a sensor or thermocouple and hence there is a loss of accuracy in the measurement, or, more simply, the surface of the body may be unsuitable for attaching a sensor to measure the temperature or the heat flux. The situation when neither the temperature nor the heat flux can be specified on a part of the boundary while both of them are known on the other part leads in the mathematical formulation to the following ill-posed problem

$$\begin{cases} LT(\bar{x}) = k_{11}\dfrac{\partial^2 T}{\partial x^2} + 2k_{12}\dfrac{\partial^2 T}{\partial x \partial y} + k_{22}\dfrac{\partial^2 T}{\partial y^2} = 0 & \bar{x} \in \Omega \\ T(\bar{x}) = f(\bar{x}) & \bar{x} \in \Gamma_1 \\ \dfrac{\partial T}{\partial \nu^+}(\bar{x}) = q(\bar{x}) & \bar{x} \in \Gamma_1 \end{cases} \tag{3}$$

where

$$\frac{\partial}{\partial \nu^+} = \sum_{i,j=1}^{2} k_{ij} \cos(\nu, x_i) \frac{\partial}{\partial x_j}, \tag{4}$$

$\cos(\nu, x_i)$ are the direction cosines of the normal vector ν to the surface Γ and f and q are prescribed functions. This problem, termed the Cauchy problem, is much more difficult to solve, both analytically and numerically, than the direct problem because the solution does not satisfy the general conditions of well-posedness. Although the problem may have a unique solution, it is well known, see e.g. Hadamard [4], that this solution is unstable with respect to small perturbations in the data on Γ_1 and thus the problem is ill posed and we cannot use the same direct approach, e.g. Gaussian elimination method, to solve the resulting system of linear equations that arise from discretising Eq. (3). It was shown by Mera et al. [9] that the Cauchy problem may be accurately solved by reducing it to a sequence of mixed well-posed problems. The numerical procedure was based on an iterative algorithm first proposed Kozlov et al. [8], which is described in Section 5. The BEM numerical implementation using constant boundary elements was investigated in detail by Mera et al. [9] and it was shown that the algorithm produces an accurate, convergent and stable numerical solution provided that a regularising stopping criterion is used. In this paper we investigate the improvement in the numerical solution obtained using higher-order boundary elements for both the Dirichlet and the Cauchy problems.

3. The boundary element method

As detailed descriptions of various BEM formulations for obtaining the solutions to the plane potential boundary value problems have been previously presented, see for example Brebbia [1], Brebbia et al. [2], Kane [7] and Paris and Canas [10], only those features necessary to facilitate a concise explanation of the modifications for the anisotropic case are presented.

One way of dealing with the anisotropicity is to transform the governing partial differential equation (1) into its canonical form by changing the spatial co-ordinates. However, after this transformation the domain deforms and rotates and the boundary conditions become, in general, more complicated than the original ones. Therefore, rather than adopt this approach we use the fundamental solution for the differential operator of the anisotropic heat conduction equation in its original form. By using the fundamental solution of the heat equation and Green's identities, the governing partial differential equation (1) is transformed into the following integral equation, see Chang et al. [3],

$$\eta(\bar{x})T(\bar{x}) = \int_{\Gamma} \left[G_2(\bar{x}, \bar{x}') \frac{\partial T}{\partial \nu^+}(\bar{x}') - T(\bar{x}') \frac{\partial G_2}{\partial \nu^+}(\bar{x}, \bar{x}') \right] \mathrm{d}\Gamma_{\bar{x}'} \tag{5}$$

where

(i) $\bar{x} \in \bar{\Omega}$, $\bar{x}' \in \Gamma$ (if smooth),
(ii) $\eta(\bar{x}) = 1$ if $\bar{x} \in \Omega$ and $\eta(\bar{x}) = 1/2$ if $\bar{x} \in \Gamma$,
(iii) $\mathrm{d}\Gamma_{\bar{x}'}$ denotes the differential increment of Γ at $\bar{x}'$,

(iv) G_2 is the fundamental solution of Eq. (1), namely,

$$G_2(\bar{x},\bar{x}') = -\frac{|k^{ij}|^{1/2}}{2\pi} \times \ln\left(\sqrt{k^{11}(x-x')^2 + 2k^{12}(x-x')(y-y') + k^{22}(y-y')^2}\right), \tag{6}$$

where k^{ij} is the inverse matrix of k_{ij} and $|k^{ij}|$ is the determinant of k^{ij}. In practice the boundary integral equation (5) can rarely be solved analytically and thus some form of numerical approximation is necessary. Therefore, the boundary of the domain is divided into N subintervals Γ_j, $j = \overline{1,N}$, and over each element Γ_j the temperature and the heat flux are approximated by various interpolation functions.

3.1. Constant boundary elements

In the BEM using constant elements (CBEM) it is assumed that the temperature and the heat flux are constant over each element Γ_j and take their values at its midpoint $\bar{\bar{x}}_j$. Using these approximations, the boundary integral equation (5) may be discretised as follows

$$\eta(\bar{x})T(\bar{x}) = \sum_{j=1}^{N} T'_j A_j(\bar{x}) - \sum_{j=1}^{N} T_j B_j(\bar{x}) \tag{7}$$

where $\bar{x}_{j-1}, \bar{x}_j$ are the end-points of the boundary element Γ_j, $T_j = T(\bar{\bar{x}}_j)$, $T'_j = (\partial T/\partial \nu^+)(\bar{\bar{x}}_j)$, $j = \overline{1,N}$, and the coefficient integrals are given by

$$A_j(\bar{x}) = A(\bar{x},\bar{x}_{j-1},\bar{x}_j) = \int_{\Gamma_j} G_2(\bar{x},\bar{x}')\,\mathrm{d}\Gamma_j(\bar{x}') \tag{8}$$

$$B_j(\bar{x}) = B(\bar{x},\bar{x}_{j-1},\bar{x}_j) = \int_{\Gamma_j} \frac{\partial}{\partial \nu^+} G_2(\bar{x},\bar{x}')\,\mathrm{d}\Gamma_j(\bar{x}') \tag{9}$$

The approximation of the boundary by straight lines enables us to evaluate analytically the integrals $A_j(\bar{x})$ and $B_j(\bar{x})$ in Eqs. (8) and (9), see Appendix A, for every $\bar{x} \in \bar{\Omega}$. For intervals other than straight lines it is seldom possible to evaluate the integrals we require analytically and thus some form of numerical quadrature must be used.

Eq. (7), applied at each of the nodal points $\bar{\bar{x}}_j, j = \overline{1,N}$, yields a system of N linear algebraic equations

$$\sum_{j=1}^{N} [G_{ij}T'_j - H_{ij}T_j] = 0 \qquad \text{for } i = \overline{1,N} \tag{10}$$

where the matrices G and H are defined by

$$G_{ij} = A_j(\bar{\bar{x}}_i);\ \ H_{ij} = B_j(\bar{\bar{x}}_i) + \tfrac{1}{2}\delta_{ij} \qquad \text{for } i,j = \overline{1,N} \tag{11}$$

and δ_{ij} is the Kronecker delta symbol. Often in practical computations N of the unknowns can be eliminated from the boundary conditions imposed and thus the problem reduces to solving a lower system of N equations with N unknowns, which can be solved by iterative or direct methods, e.g. Gaussian elimination.

The main source of errors in the method described is in the approximation of each unknown boundary function by a step-function, the application of the resulting boundary integral equation at a finite number of points and the approximation (where necessary) of the coefficient integrals in the resulting system of linear algebraic equations. Compared with these, the errors arising from the solution of the linear system of equations are usually negligible and may therefore be ignored. Thus, the accuracy of the method described clearly depends upon how well the unknown function and its normal derivative can be represented by constants in each interval of the boundary and this, in turn, depends to some extent upon the lengths of the intervals into which the boundary is divided. It follows that if either T or $(\partial T/\partial \nu^+)$ changes rapidly along the boundary, then more intervals are generally required than would otherwise be the case. However, if the rapid variation is confined to a particular part of the boundary, we may economise in computer time and storage by dividing only that part of the boundary into finer intervals and thus use boundary elements of different lengths. If the total number of boundary intervals is severely limited by computer storage capacity, improved results with a smaller number of intervals may be obtained by using more accurate representations for T and $(\partial T/\partial \nu^+)$, e.g. higher-order interpolation functions.

3.2. Linear boundary elements

The linear boundary element method (LBEM) affords a more accurate approximation of Green's Integral Formula (5) than the classical CBEM. On each boundary element Γ_j the temperature and the heat flux are approximated by piecewise linear functions

$$T(\bar{x}) = (1-\zeta)T(\bar{x}_{j-1}) + \zeta T(\bar{x}_j) \qquad \text{for } \bar{x} \in \Gamma_j \tag{12}$$

$$T'(\bar{x}) = (1-\zeta)T'(\bar{x}_{j-1}) + \zeta T'(\bar{x}_j) \qquad \text{for } \bar{x} \in \Gamma_j \tag{13}$$

where $\bar{x}_{j-1}$ and $\bar{x}_j$ are the end-points of Γ_j and ζ is the natural co-ordinate along the element, which increases from zero at $\bar{x}_{j-1}$ to unity at $\bar{x}_j$. Correspondingly, the boundary integral equation (5) becomes

$$\eta(\bar{x})T(\bar{x}) = \sum_{j=1}^{N} T'_{j-1}[A_j(\bar{x}) - C_j(\bar{x})] + \sum_{j=1}^{N} T'_j C_j(\bar{x}) - \sum_{j=1}^{N} T_{j-1}[B_j(\bar{x}) - D_j(\bar{x})] - \sum_{j=1}^{N} T_j D_j(\bar{x}) \tag{14}$$

where

- $T_j = T(\bar{x}_j)$, $T'_j = (\partial T/\partial \nu^+)(\bar{x}_j)$ for $j = \overline{0,N}$;
- the coefficients $A_j(\bar{x})$ and $B_j(\bar{x})$ have the same meaning as for the constant element case, see Eqs. (8) and (9);

- the coefficients $C_j(\bar{x})$ and $D_j(\bar{x})$ are given by

$$C_j(\bar{x}) = C(\bar{x}, \bar{x}_{j-1}, \bar{x}_j) = \int_{\Gamma_j} G_2(\bar{x}, \bar{x}')\zeta \, \mathrm{d}\Gamma_j(\bar{x}') \tag{15}$$

$$D_j(\bar{x}) = D(\bar{x}, \bar{x}_{j-1}, \bar{x}_j) = \int_{\Gamma_j} \frac{\partial}{\partial \nu^+} G_2(\bar{x}, \bar{x}')\zeta \, \mathrm{d}\Gamma_j(\bar{x}') \tag{16}$$

and may be evaluated analytically, see Appendix A.

In the LBEM the collocation points, i.e. the points where the discretised boundary integral equation (14) is applied on the boundary, are taken to be the interval end-points $\bar{x}_j, j = \overline{1,N}$, rather than at the nodal points $\bar{\tilde{x}}_j, j = \overline{1,N}$, as in the CBEM. Eq. (14) applied at each of the interval points $\bar{x}_j, j = \overline{1,N}$, yields a system of N linear algebraic equations

$$\sum_{j=1}^{N} (G_{ij}T'_j - H_{ij}T_j) = 0 \qquad \text{for } i = \overline{1,N} \tag{17}$$

where the matrices G and H are defined by

$$G_{ij} = -[A_{j+1}(\bar{x}_i) - C_{j+1}(\bar{x}_i)] - C_j(\bar{x}_i) \qquad \text{for } i,j = \overline{1,N} \tag{18}$$

$$H_{ij} = -[B_{j+1}(\bar{x}_i) - D_{j+1}(\bar{x}_i)] - D_j(\bar{x}_i) \quad \text{for } i,j = \overline{1,N},\ i \neq j \tag{19}$$

The diagonal coefficients of the matrix H may be evaluated using the fact that when a uniform temperature $T = c$ is applied over the whole boundary then the normal derivative must be zero and Eq. (17) becomes

$$\sum_{j=1}^{N} H_{ij}c = 0 \qquad \text{for } i = \overline{1,N} \tag{20}$$

Thus the sum of all the elements of H in any row ought to be zero, and the value of the coefficient on the diagonal can be easily calculated once the off-diagonal coefficients are all known, i.e.

$$H_{ii} = -\sum_{j \neq i} H_{ij} \qquad \text{for } i = \overline{1,N} \tag{21}$$

3.3. Quadratic boundary elements

A more accurate approximation of the solution of the boundary integral equation (5) can be obtained using the quadratic boundary element method (QBEM). In this approach, on each boundary element Γ_j the temperature and the heat flux are approximated by quadratic functions, namely,

$$T(\bar{x}) = N_1(\zeta)T_{2j-1} + N_2(\zeta)T_{2j} + N_3(\zeta)T_{2j+1} \tag{22}$$

$$T'(\bar{x}) = N_1(\zeta)T'_{2j-1} + N_2(\zeta)T'_{2j} + N_3(\zeta)T'_{2j+1} \tag{23}$$

where $T_{2j-1} = T(\bar{x}_{j-1})$, $T_{2j} = T(\bar{\tilde{x}}'_j)$, $T_{2j+1} = T(\bar{x}_j)$, $T'_{2j-1} = (\partial T/\partial \nu^+)(\bar{x}_{j-1})$, $T'_{2j} = (\partial T/\partial \nu^+)(\bar{\tilde{x}}_j)$, $T'_{2j+1} = (\partial T/\partial \nu^+)(\bar{x}_j)$, ζ is the natural co-ordinate along the element Γ_j taking value zero at $\bar{x}_{j-1}$, one half at $\bar{\tilde{x}}_j$ and unity at $\bar{x}_j$. The shape functions N_i, $i = \overline{1,3}$ are given by

$$N_1(\zeta) = (\zeta - 1)(2\zeta - 1), \qquad N_2(\zeta) = 4\zeta(1 - \zeta), \qquad N_3(\zeta) = \zeta(2\zeta - 1) \tag{24}$$

On the basis of these approximations the boundary integral equation (5) becomes

$$\begin{aligned}\eta(\bar{x})T(\bar{x}) = &\sum_{j=1}^{N} T'_{2j-1}[2E_j(\bar{x}) - 3C_j(\bar{x}) + A_j(\bar{x})] \\ &+ \sum_{j=1}^{N} T'_{2j}[-4E_j(\bar{x}) + 4C_j(\bar{x})] \\ &+ \sum_{j=1}^{N} T'_{2j+1}[2E_j(\bar{x}) - C_j(\bar{x})] \\ &- \sum_{j=1}^{N} T_{2j-1}[2F_j(\bar{x}) - 3D_j(\bar{x}) + B_j(\bar{x})] \\ &- \sum_{j=1}^{N} T_{2j}[-4F_j(\bar{x}) + 4D_j(\bar{x})] \\ &- \sum_{j=1}^{N} T_{2j+1}[2F_j(\bar{x}) - D_j(\bar{x})]\end{aligned} \tag{25}$$

where

- the coefficients $A_j(\bar{x})$ and $B_j(\bar{x})$ have the same meaning as for the constant element case, see Eqs. (8) and (9);
- the coefficients $C_j(\bar{x})$ and $D_j(\bar{x})$ have the same meaning as for the linear element case, see Eqs. (15) and (16);
- the coefficients $E_j(\bar{x})$ and $F_j(\bar{x})$ are given by

$$E_j(\bar{x}) = E(\bar{x}, \bar{x}_{j-1}, \bar{x}_j) = \int_{\Gamma_j} G_2(\bar{x}, \bar{x}')\zeta^2 \, \mathrm{d}\Gamma_j(\bar{x}') \tag{26}$$

$$F_j(\bar{x}) = F(\bar{x}, \bar{x}_{j-1}, \bar{x}_j) = \int_{\Gamma_j} \frac{\partial}{\partial \nu^+} G_2(\bar{x}, \bar{x}')\zeta^2 \, \mathrm{d}\Gamma_j(\bar{x}') \tag{27}$$

and may be evaluated analytically, see Appendix A.

In the QBEM the discretised boundary integral equation (25) is applied on the boundary at every nodal point $\bar{\tilde{x}}_j, j = \overline{1,N}$ and every interval end point $\bar{x}_j, j = \overline{1,N}$, a system of $2N$ linear algebraic equations

$$\sum_{j=1}^{2N} (G_{ij}T'_j - H_{ij}T_j) = 0 \qquad \text{for } i = \overline{1,2N} \tag{28}$$

is obtained, where the matrices G and H are defined by

$$G_{i,2j} = -4E_j(\bar{z}_i) + 4C_j(\bar{z}_i) \qquad \text{for } i = \overline{1,2N}\ \ j = \overline{1,N} \tag{29}$$

$$G_{i,2j-1} = [2E_j(\bar{z}_i) - 3C_j(\bar{z}_i) + A_j(\bar{z}_i)] + [2E_{j-1}(\bar{z}_i) - C_{j-1}(\bar{z}_i)]$$

for $i = \overline{1,2N}$ $j = \overline{1,N}$

$$H_{i,2j} = -4F_j(\bar{z}_i) + 4D_j(\bar{z}_i) \quad \text{for } i = \overline{1,2N}\ j = \overline{1,N},\ i \neq 2j \tag{31}$$

$$H_{i,2j-1} = [2F_j(\bar{z}_i) - 3D_j(\bar{z}_i) + B_j(\bar{z}_i)] + [2F_{j-1}(\bar{z}_i) - D_{j-1}(\bar{z}_i)]$$

for $i = \overline{1,2N}$ $j = \overline{1,N}$, $i \neq 2j-1$

and the collocation points $\bar{z}_i$, $i = 1, 2N$ are given by

$$\bar{z}_{2i-1} = \bar{x}_{i-1}\ \ \bar{z}_{2i} = \tilde{\bar{x}}_i \qquad i = \overline{1,N} \tag{33}$$

The diagonal coefficients of the matrix H are evaluated by assuming a constant temperature case, as for the LBEM. We note that for a boundary element discretisation with N boundary elements, the QBEM requires the solution of $2N$ equations in $2N$ unknowns, whereas the CBEM and the LBEM both require the solution of N equations in N unknowns.

3.4. Discontinuous boundary elements

We note that with the classical CBEM, nodal points are situated only at the segment mid-points and therefore the heat flux ($\partial T/\partial \nu^+$) has precisely one value at each of these nodal points. However, with the linear and the quadratic BEM formulations presented in the previous sections, nodes are situated at segment end-points and therefore, if the domain has corners, at those points the heat flux has two components, one related to each of the sides adjacent to the corner. The same problem arises if discontinuous or singular boundary conditions are prescribed. Therefore, in order to deal with corners, discontinuities and singularities, discontinuous linear and quadratic boundary elements are introduced in this section.

As with continuous linear elements (LBEM) in the discontinuous linear elements method (DLBEM) it is assumed that the variables in the integral equation (5) have a linear evolution along the elements. These boundary elements are also segments of a straight line, the difference with respect to LBEM being that the linear evolution is expressed through the values of the functions at two internal points given by

$$\bar{x}^j_{\alpha,1} = (1-\alpha)\bar{x}_{j-1} + \alpha\bar{x}_j \tag{34}$$

$$\bar{x}^j_{\alpha,2} = \alpha\bar{x}_{j-1} + (1-\alpha)\bar{x}_j \tag{35}$$

where $\alpha \in (0, 1/2)$. The temperature and the heat flux are approximated by

$$T(\bar{x}) = (1-\zeta)T(\bar{x}^j_{\alpha,1}) + \zeta T(\bar{x}^j_{\alpha,2}) \qquad \text{for } \bar{x} \in \Gamma_j \tag{36}$$

$$T'(\bar{x}) = (1-\zeta)T'(\bar{x}^j_{\alpha,1}) + \zeta T'(\bar{x}^j_{\alpha,2}) \qquad \text{for } \bar{x} \in \Gamma_j \tag{37}$$

where $\bar{x}_{j-1}$ and $\bar{x}_j$ are the end-points of Γ_j and ζ is the natural co-ordinate along the element, which increases from zero at $\bar{x}_{j-1}$ to unity at $\bar{x}_j$. Correspondingly, the boundary integral equation (5) becomes

$$\begin{aligned}\eta(\bar{x})T(\bar{x}) = &\sum_{j=1}^{N} T'_{2j-1}\left[\frac{1-\alpha}{1-2\alpha}A_j(\bar{x}) - \frac{1}{1-2\alpha}C_j(\bar{x})\right] \\ &+ \sum_{j=1}^{N} T'_{2j}\left[\frac{1}{1-2\alpha}C_j(\bar{x}) - \frac{\alpha}{1-2\alpha}A_j(\bar{x})\right] \\ &- \sum_{j=1}^{N} T_{2j-1}\left[\frac{1-\alpha}{1-2\alpha}B_j(\bar{x}) - \frac{1}{1-2\alpha}D_j(\bar{x})\right] \\ &- \sum_{j=1}^{N} T_{2j}\left[\frac{1}{1-2\alpha}D_j(\bar{x}) - \frac{\alpha}{1-2\alpha}B_j(\bar{x})\right]\end{aligned} \tag{38}$$

where A_j, B_j, C_j and D_j have the same meaning as in Section 3.2 and $T_{2j-1} = T(\bar{x}^j_{\alpha,1})$, $T_{2j} = T(\bar{x}^j_{\alpha,2})$, $T'_{2j-1} = (\partial T/\partial \nu^+)\times(\bar{x}^j_{\alpha,1})$, $T'_{2j} = (\partial T/\partial \nu^+)(\bar{x}^j_{\alpha,2})$ for $j = \overline{1,N}$. In the DLBEM the discretised boundary integral equation (38) is applied on the boundary at each of the points $\bar{x}^j_{\alpha,1}, \bar{x}^j_{\alpha,2}, j = \overline{1,N}$, leading to a system of $2N$ equations

$$\sum_{j=1}^{2N}(G_{ij}T'_j - H_{ij}T_j) = 0 \qquad \text{for } i = \overline{1,2N} \tag{39}$$

where the matrices G_{ij} and H_{ij} are given by

$$G_{i,2j-1} = \frac{1-\alpha}{1-2\alpha}A_j(\bar{z}_i) - \frac{1}{1-2\alpha}C_j(\bar{z}_i) \quad \text{for } i = \overline{1,2N},\ j = \overline{1,N} \tag{40}$$

$$G_{i,2j} = \frac{1}{1-2\alpha}C_j(\bar{z}_i) - \frac{\alpha}{1-2\alpha}A_j(\bar{z}_i) \quad \text{for } i = \overline{1,2N},\ j = \overline{1,N} \tag{41}$$

$$H_{i,2j-1} = \frac{1-\alpha}{1-2\alpha}B_j(\bar{z}_i) - \frac{1}{1-2\alpha}D_j(\bar{z}_i) \quad \text{for } i = \overline{1,2N},\ j = \overline{1,N}\ i \neq 2j-1 \tag{42}$$

$$H_{i,2j} = \frac{1}{1-2\alpha}D_j(\bar{z}_i) - \frac{\alpha}{1-2\alpha}B_j(\bar{z}_i) \quad \text{for } i = \overline{1,2N},\ j = \overline{1,N}\ i \neq 2j \tag{43}$$

and the collocation points $\bar{z}_i$, $i = 1, 2N$ are given by

$$\bar{z}_{2i-1} = \bar{x}^i_{\alpha,1} \;\; \bar{z}_{2i} = \bar{x}^i_{\alpha,2} \qquad i = \overline{1,N} \tag{44}$$

The diagonal coefficients of the matrix H are evaluated by assuming a constant temperature case, as for the LBEM.

In a similar way to the QBEM, in the DQBEM the temperature and the heat flux are assumed to have a quadratic evolution along the elements but this evolution is expressed through the values at three internal points, namely, $\bar{x}^j_{\alpha,1}$, $\bar{x}^j_{\alpha,2}$ and $\tilde{\bar{x}}_j$, $j = \overline{1,N}$. Thus the temperature and the heat flux are approximated as

$$T(\bar{x}) = N_1(\zeta)T_{3j-2} + N_2(\zeta)T_{3j-1} + N_3(\zeta)T_{3j} \tag{45}$$

$$T'(\bar{x}) = N_1(\zeta)T'_{3j-2} + N_2(\zeta)T'_{3j-1} + N_3(\zeta)T'_{3j} \tag{46}$$

where $T_{3j-2} = T(\bar{x}^j_{\alpha,1})$, $T_{3j-1} = T(\tilde{\bar{x}}_j)$, $T_{3j} = T(\bar{x}^j_{\alpha,2})$, $T'_{3j-2} = (\partial T/\partial \nu^+)(\bar{x}^j_{\alpha,1})$, $T'_{3j-1} = (\partial T/\partial \nu^+)(\tilde{\bar{x}}_j)$, $T'_{3j} = (\partial T/\partial \nu^+)(\bar{x}^j_{\alpha,2})$, ζ is the natural co-ordinate along the element Γ_j taking value zero at $\bar{x}_{j-1}$, one half at $\tilde{\bar{x}}_j$ and unity at $\bar{x}_j$. The shape functions N_i, $i = \overline{1,3}$ are given by

$$N_1(\zeta) = \frac{2\zeta^2 - (3-2\alpha)\zeta + 1 - \alpha}{(2\alpha-1)^2} \tag{47}$$

$$N_2(\zeta) = -\frac{-4\zeta^2 - 4\zeta + 4\alpha(1-\alpha)}{(2\alpha-1)^2} \tag{48}$$

$$N_3(\zeta) = \frac{2\zeta^2 - (1+2\alpha)\zeta + \alpha}{(2\alpha-1)^2} \tag{49}$$

On the basis of these approximations the boundary integral equation (5) becomes

$$\begin{aligned}
\eta(\bar{x})T(\bar{x}) = {} & \sum_{j=1}^{N} T'_{3j-2}\left[\frac{1-\alpha}{(2\alpha-1)^2}A_j(\bar{x}) + \frac{2\alpha-3}{(2\alpha-1)^2}C_j(\bar{x}) + \frac{2}{(2\alpha-1)^2}E_j(\bar{x})\right] \\
& + \sum_{j=1}^{N} T'_{3j-1}\left[\frac{4\alpha(\alpha-1)}{(2\alpha-1)^2}A_j(\bar{x}) + \frac{4}{(2\alpha-1)^2}C_j(\bar{x}) - \frac{4}{(2\alpha-1)^2}E_j(\bar{x})\right] + \sum_{j=1}^{N} T'_{3j}\left[\frac{\alpha}{(2\alpha-1)^2}A_j(\bar{x}) - \frac{1+2\alpha}{(2\alpha-1)^2}C_j(\bar{x}) + \frac{2}{(2\alpha-1)^2}E_j(\bar{x})\right] \\
& - \sum_{j=1}^{N} T_{3j-2}\left[\frac{1-\alpha}{(2\alpha-1)^2}B_j(\bar{x}) + \frac{2\alpha-3}{(2\alpha-1)^2}D_j(\bar{x}) + \frac{2}{(2\alpha-1)^2}F_j(\bar{x})\right] \\
& - \sum_{j=1}^{N} T_{3j-1}\left[\frac{4\alpha(\alpha-1)}{(2\alpha-1)^2}B_j(\bar{x}) + \frac{4}{(2\alpha-1)^2}D_j(\bar{x}) - \frac{4}{(2\alpha-1)^2}F_j(\bar{x})\right] - \sum_{j=1}^{N} T_{3j}\left[\frac{\alpha}{(2\alpha-1)^2}B_j(\bar{x}) - \frac{1+2\alpha}{(2\alpha-1)^2}D_j(\bar{x}) + \frac{2}{(2\alpha-1)^2}F_j(\bar{x})\right]
\end{aligned} \tag{50}$$

where the coefficients A_j, B_j, C_j, D_j, E_j and F_j are evaluated analytically by the formulae given in Appendix A. In the DQBEM the discretised boundary integral equation (50) is applied on each boundary element Γ_j at three points, namely, $\bar{x}^j_{\alpha,1}$, $\bar{x}^j_{\alpha,2}$ and $\tilde{\bar{x}}_j$, $j = \overline{1,N}$ leading to a system of $3N$ linear equations

$$\sum_{j=1}^{3N}(G_{ij}T'_j - H_{ij}T_j) = 0 \qquad \text{for } i = \overline{1,3N} \tag{51}$$

where the matrices G_{ij} and H_{ij} are given by

$$G_{i,3j-2} = \frac{1-\alpha}{(2\alpha-1)^2}A_j(\bar{z}_i) + \frac{2\alpha-3}{(2\alpha-1)^2}C_j(\bar{z}_i) + \frac{2}{(2\alpha-1)^2}E_j(\bar{z}_i) \tag{52}$$

$$G_{i,3j-1} = \frac{4\alpha(\alpha-1)}{(2\alpha-1)^2}A_j(\bar{z}_i) + \frac{4}{(2\alpha-1)^2}C_j(\bar{z}_i) - \frac{4}{(2\alpha-1)^2}E_j(\bar{z}_i) \tag{53}$$

$$G_{i,3j} = \frac{\alpha}{(2\alpha-1)^2}A_j(\bar{z}_i) - \frac{1+2\alpha}{(2\alpha-1)^2}C_j(\bar{z}_i) + \frac{2}{(2\alpha-1)^2}E_j(\bar{z}_i) \tag{54}$$

$$\text{for } i = \overline{1,3N}, \qquad j = \overline{1,N} \tag{55}$$

$$H_{i,3j-2} = \frac{1-\alpha}{(2\alpha-1)^2}B_j(\bar{z}_i) + \frac{2\alpha-3}{(2\alpha-1)^2}D_j(\bar{z}_i) + \frac{2}{(2\alpha-1)^2}F_j(\bar{z}_i) \tag{56}$$

$$\text{for } i = \overline{1,3N}, \qquad j = \overline{1,N} \qquad i \neq 3j-2 \tag{57}$$

$$H_{i,3j-2} = \frac{4\alpha(\alpha-1)}{(2\alpha-1)^2}B_j(\bar{z}_i) + \frac{4}{(2\alpha-1)^2}D_j(\bar{z}_i) - \frac{4}{(2\alpha-1)^2}F_j(\bar{z}_i) \tag{58}$$

$$\text{for } i = \overline{1,3N}, \qquad j = \overline{1,N} \qquad i \neq 3j-1 \tag{59}$$

$$H_{i,3j} = \frac{\alpha}{(2\alpha-1)^2} B_j(\bar{z}_i) - \frac{1+2\alpha}{(2\alpha-1)^2} D_j(\bar{z}_i) + \frac{2}{(2\alpha-1)^2} F_j(\bar{z}_i) \tag{60}$$

$$\text{for } i = \overline{1,3N}, \qquad j = \overline{1,N} \qquad i \neq 3j \tag{61}$$

and the collocation points $\bar{z}_i$, $i = 1, 3N$ are given by

$$\bar{z}_{3i-2} = \bar{x}^i_{\alpha,1}, \;\; \bar{z}_{3i-1} = \tilde{\bar{x}}_i, \;\; \bar{z}_{3i} = \bar{x}^i_{\alpha,2} \qquad i = \overline{1,N} \tag{62}$$

The diagonal coefficients of the matrix H are evaluated by assuming a constant temperature case, as for the LBEM.

Thus, for a boundary element discretisation with N boundary elements, the CBEM and LBEM require the solution of N equations in N unknowns, the QBEM and DLBEM require the solution of $2N$ equations in $2N$ unknowns whilst the DQBEM requires the solution of $3N$ equations in $3N$ unknowns. The comparison in terms of accuracy cannot be maintained in terms of the number of boundary elements, but rather in terms of the size of the system of equations. We note that discontinuous BEMs require the solution of a larger system of equations but they can be used to deal with corners and discontinuities, see Kane [7], Patterson and Sheikh [11] and Subia et al. [12]. They are also particularly well suited to modelling singular fields, see Paris and Canas [10].

The analytical evaluation of the integrals associated with CBEM, LBEM, QBEM for the isotropic case were presented by Ingham et al. [5]. However, the integrals associated with the BEM for anisotropic heat conduction problems are not available in the literature and have previously been evaluated numerically.

Evaluation of these integrals by the analytical expressions given in Appendix A requires only a fraction of the computational time taken by an accurate numerical technique. In addition, since for a boundary element discretisation with N boundary elements each of these integrals has to be evaluated N times at every point to which Green's Integral Formula is applied, these analytical expressions yield appreciable reductions in the computational times required by the BEMs.

4. Numerical results obtained for the Dirichlet problem

It is the purpose of this section to illustrate and compare the accuracy and the convergence of the BEMs described in Sections 3.1–3.4 when applied to solve the Dirichlet problem (2). In order to illustrate typical numerical results we consider an anisotropic medium with the thermal conductivity tensor k_{ij} given by

$$k_{11} = 5.0, \qquad k_{12} = k_{21} = 2.0, \qquad k_{22} = 1.0 \tag{63}$$

and the analytical temperature distribution to be retrieved given by

$$T(x,y) = \frac{x^3}{5} - x^2 y + xy^2 + \frac{y^3}{3} \tag{64}$$

The test example expressed by Eqs. (63) and (64) was chosen such that the exact solution for the temperature is not a constant, linear or quadratic function since our aim is to compare the efficiency of approximating an arbitrary function by piecewise constant, linear or quadratic functions.

The most significant quantity to characterise the anisotropy of a media is the determinant of the conductivity coefficients, i.e. $|k_{ij}| = k_{11}k_{22} - k_{12}^2$. The smaller is the value of $|k_{ij}|$, the more asymmetric are the temperature fields and the heat flux vectors. Since the criterion $|k_{ij}| > 0$ determines the type of the differential equation, parabolic for transient problems and elliptic for steady problems, therefore, the smaller the value of $|k_{ij}|$, the more difficult is the numerical calculation, see Chang et al. [3]. The test example of Eqs. (63) and (64) also ensures that the determinant of the thermal conductivity tensor is not too small in order to maintain reasonable accuracy. Numerous other examples for anisotropic media with different thermal conductivity tensors have been investigated but the same conclusions as those obtained using the test example expressed by Eqs. (63) and (64) were drawn.

Both the Dirichlet and the Cauchy problems are solved in the plane domain $\Omega = \{(x,y) : x^2 + y^2 < 1\}$, i.e. the two-dimensional disc of radius unity. The boundary of the domain $\Gamma = \{(x,y) | x^2 + y^2 = 1\}$ is divided into N subintervals Γ_j, $j = 1, \ldots, N$. The end-points of these boundary elements are taken to be equally spaced on the boundary Γ, starting from the point $\bar{x} = (1.0, 0.0)$. Various numbers of boundary elements, $N \in \{40, 60, 80, 120\}$ were used to obtain the numerical solutions presented in this paper. In the solution domain the temperature was evaluated at various arbitrary points. In order to illustrate the typical results that we have obtained we present the numerical solution at the point $\bar{x}_0 = (0.25, 0.25)$.

By solving the system of linear algebraic equations (10), (17), (28), (39) or (51) obtained by applying the various BEMs described in Sections 3.1–3.4 the values of the heat flux $(\partial T/\partial \nu^+)$ on the boundary are established. Once these heat flux values have been obtained the BEM can be explicitly used to determine the temperature inside the solution domain using Eqs. (7), (14), (25), (38) or (50).

The numerical results for the temperature at the interior point $\bar{x}_0 = (0.25, 0.25)$ obtained using $N \in \{40, 60, 80\}$ boundary elements for the CBEM, LBEM, DLBEM, QBEM and DQBEM are presented in Tables 1 and 2 in comparison with the exact solution, together with the percentage error. It can be seen that for all the methods considered the error in predicting the exact solution decreases as the number of boundary elements is increased and for large numbers of boundary elements the agreement between the numerical and the exact solution is very good. Similar results are obtained for any point inside the solution

Table 1
The percentage error in predicting the exact solution for the temperature at the internal point $\bar{x}_0 = (0.25, 0.25)$ obtained with various numbers of boundary element $N \in \{40, 60, 80\}$, for: (a) CBEM, (b) LBEM and (c) DLBEM for the Dirichlet problem given by Eq. (2)

N	Analytical solution	Numerical solution	Percentage error (%)
(a) CBEM			
40	0.008333	0.008835	6.016
60	0.008333	0.008537	2.446
80	0.008333	0.008436	1.234
(b) LBEM			
40	0.008333	0.009198	10.378
60	0.008333	0.008708	4.496
80	0.008333	0.008539	2.471
(c) DLBEM			
40	0.008333	0.008244	1.071
60	0.008333	0.008288	0.544
80	0.008333	0.008308	0.298

domain Ω. Therefore, it can be concluded that all the BEMs described in this chapter produce a numerical solution that is accurate and convergent with respect to the increasing number of boundary elements.

The numerical results presented in this paper for DLBEM and DQBEM are obtained for the two collocation points $\bar{x}^j_{\alpha,1}$ and $\bar{x}^j_{\alpha,2}$ placed at a quarter of the segment length from the boundary edges, i.e. α is taken to be 0.25 in Eqs. (34) and (35). Table 3 shows, for various values of α, the percentage errors in evaluating the temperature at the point $\bar{x}_0 = (0.25, 0.25)$ by DLBEM and DQBEM with $N = 40$ boundary elements. It can be seen that accurate results are obtained over a large range of α values. However, if α is too close to the extreme values 0 or 1/2, i.e. if the two collocation points $\bar{x}^j_{\alpha,1}$ and $\bar{x}^j_{\alpha,2}$ are too close to the end-point of the boundary elements or too close to each other, then the accuracy of the numerical solution is reduced.

However, even if extreme values are used for α, an accurate numerical solution is obtained provided that the number of boundary elements is large enough. For example, for $\alpha = 0.05$ and $\alpha = 0.45$ the errors in predicting the temperature at the point x_0 are 7.88 and 5.15%, respectively, if a DLBEM with $N = 40$ boundary elements is used, see Table 3. It was found that if the number of boundary elements is increased to $N = 160$ then the errors at the point x_0 are reduced to 0.43 and 0.25% for $\alpha = 0.05$ and $\alpha = 0.45$, respectively. Thus accurate solutions may be obtained for any value of the parameter $\alpha \in (0, 1/2)$.

Table 2
The percentage error in predicting the exact solution for the temperature at the internal point $\bar{x}_0 = (0.25, 0.25)$ obtained with various numbers of boundary element $N \in \{40, 60, 80\}$, for: (a) QBEM and (b) DQBEM for the Dirichlet problem given by Eq. (2)

N	Analytical solution	Numerical solution	Percentage error (%)
(a) QBEM			
40	0.008333	0.008261	0.863
60	0.008333	0.008314	0.237
80	0.008333	0.008325	0.099
(b) DQBEM			
40	0.008333	0.008333	0.009
60	0.008333	0.008333	0.002
80	0.008333	0.008333	0.001

Table 3
The percentage error in predicting the exact solution $T = 0.008333$ for the temperature at the point x_0 using DLBEM and DQBEM with $N = 40$ boundary elements for various values of the parameter α

α	DLBEM	DQBEM
0.05	7.8826	0.007
0.10	5.2669	0.002
0.15	2.8796	0.002
0.16	2.4331	0.003
0.17	1.9975	0.004
0.18	1.5731	0.004
0.19	1.1600	0.005
0.20	0.7585	0.006
0.21	0.3686	0.007
0.22	0.0094	0.007
0.23	0.3753	0.008
0.24	0.7291	0.008
0.25	1.0706	0.009
0.30	2.5888	0.011
0.35	3.7824	0.013
0.40	4.6417	0.015
0.45	5.1598	0.016

However, in order to obtain highly accurate solutions with modest numbers of boundary element the extreme values of the intervals (0, 1/2) should be avoided. Table 3 shows that for the test example considered in this section the optimum values of α are 0.22 for DLBEM and 0.15 for DQBEM. Numerous other test examples have been investigated and it was found that in general the optimum value of the parameter α is likely to occur in the interval (0.10, 0.25). Therefore, in order to obtain accurate results the collocation points $\bar{x}^j_{\alpha,1}$ and $\bar{x}^j_{\alpha,2}$ should be taken at 10–25% from the end-points of each boundary element.

In order to compare the accuracy and the convergence of the various methods employed, Table 4 presents the numerical solution for the temperature at three different internal points, obtained with the same number of boundary elements for various BEMs. It can be seen that the QBEM and the DQBEM provide more accurate results than the CBEM, LBEM or DLBEM. It is worth noting that for some domain points the LBEM produces less accurate results than the CBEM. The errors in the LBEM and the CBEM have been investigated in detail. It was found that the LBEM produces poor results for test examples for which the temperature along some of the boundary elements has a similar shape to that illustrated in Fig. 1, which presents the temperature, its constant and its linear approximations as functions of ζ, over a typical boundary element. If this temperature is multiplied by the normal derivative of Green's function, $(\partial G_2/\partial \nu^+)$, it changes its shape to that

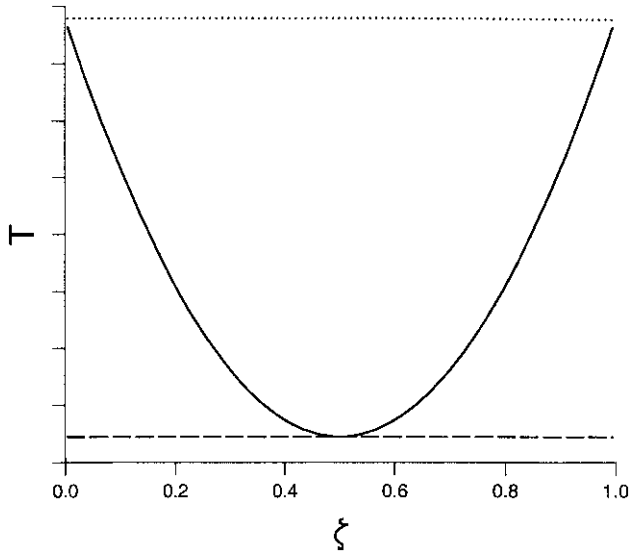

Fig. 1. The temperature (—), the constant approximation (- - -) and the linear approximation (···) over a typical boundary element.

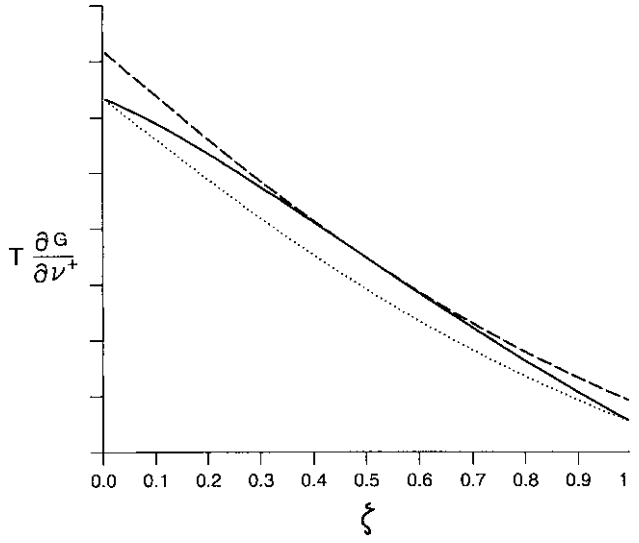

Fig. 2. The product between the normal derivative of the fundamental solution and the temperature (—), its constant approximation (- - -) and its linear approximation (···) over a typical boundary element.

presented in Fig. 2. Hence, if the integral of this product is needed it is obvious that the result is more accurate if a constant approximation is used for the temperature over this particular boundary element. If this happens for many of the boundary elements used to discretise the boundary of the solution domain, then the numerical solution produced by the LBEM is poorer than that produced by the CBEM. Numerous test examples have been investigated and it was found that the accuracy of the LBEM in comparison with the CBEM is problem dependent, while QBEM and DQBEM were always found to produce more accurate results than those obtained using constant or linear boundary elements.

We note that the numerical results presented in Table 4 are obtained for all the methods with the same number of boundary elements, namely $N = 40$. Table 5 presents the numerical results for the temperature at the point $\bar{x}_0 = (0.25, 0.25)$ obtained by solving a system of 120 equations with 120 unknowns, for each of the BEMs considered. It should be noted that the number of boundary elements is smaller, hence the errors in approximating the boundary by a polygonal line are larger, for higher-order boundary

Table 4
The percentage error in predicting the exact solution for the temperature at the internal points: (a) $\bar{x}_0 = (0.5, 0.5)$, (b) $\bar{x}_1 = (0.25, 0.25)$ and (c) $\bar{x}_2 = (0.1, 0.1)$ obtained with $N = 40$ boundary elements, for the Dirichlet problem given by Eq. (2)

Method	Analytical solution	Numerical solution	Percentage error (%)
(a) $\bar{x}_0 = (0.5,0.5)$			
CBEM	0.066667	0.069464	4.197
LBEM	0.066667	0.067992	1.988
DLBEM	0.066667	0.066499	0.252
QBEM	0.066667	0.066568	0.147
DQBEM	0.066667	0.066667	0.003
(b) $\bar{x}_1 = (0.25,0.25)$			
CBEM	0.008333	0.008835	6.016
LBEM	0.008333	0.009219	10.633
DLBEM	0.008333	0.008244	1.071
QBEM	0.008333	0.008266	0.813
DQBEM	0.008333	0.008333	0.009
(c) $\bar{x}_2 = (0.1,0.1)$			
CBEM	0.000533	0.000761	42.683
LBEM	0.000533	0.000902	69.204
DLBEM	0.000533	0.000489	8.364
QBEM	0.000533	0.000503	5.703
DQBEM	0.000533	0.000533	0.059

Table 5
The percentage error in predicting the exact solution for the temperature at the internal point $\bar{x}_0 = (0.25, 0.25)$ obtained using various BE methods, by solving a system of linear algebraic equations of size 120×120, for the Dirichlet problem given by Eq. (2)

Method	N	Analytical solution	Numerical solution	Percentage error (%)
CBEM	120	0.008333	0.008377	0.519
LBEM	120	0.008333	0.008383	0.598
DLBEM	60	0.008333	0.008288	0.598
QBEM	60	0.008333	0.008314	0.237
DQBEM	40	0.008333	0.008333	0.009

elements. However, the QBEMs produce more accurate results than constant or linear methods. As mentioned above, for some particular examples the linear elements may be less accurate than the constant elements. It should be noted also that the discontinuous boundary elements were found to provide more accurate results than their corresponding continuous boundary elements.

Numerous other test examples were investigated and similar results were obtained. Therefore, it may be concluded that all the BEMs described in this chapter produce accurate and convergent numerical solutions. However, the numerical results are substantially improved by using the quadratic boundary element methods (QBEM and DQBEM), while the linear boundary elements may produce less accurate results than constant boundary elements. Therefore, if a highly accurate solution is needed, then quadratic boundary elements should be used. In addition, the discontinuous quadratic elements, DQBEM, can also be used to deal with corners and discontinuities, see Kane [7]. We note that the use of the analytical expressions given in Appendix A for the coefficient integrals instead of quadrature formulae not only reduces the programming complexity but also results in substantial reductions in the computational time for all the methods considered in this paper.

5. Numerical procedure and results obtained for the Cauchy problem

Since the Cauchy problem (3) is highly ill-posed, standard numerical techniques were found to produce highly unstable numerical solutions. Therefore, in this section the Cauchy problem is solved by reduction to a sequence of well-posed problems. The algorithm was first proposed by Kozlov et al. [8] and consists of the following steps:

Step 1. Specify an initial boundary temperature guess u_0 on Γ_0 and solve the mixed problem

$$LT^{(0)} = 0 \text{ on } \Omega, \qquad \frac{\partial T^{(0)}}{\partial \nu^+} = q \text{ on } \Gamma_1, \qquad T^{(0)} = u_0 \text{ on } \Gamma_0 \tag{65}$$

to determine the initial approximation $T^{(0)}$ for the solution of the problem and $\mu_0 = (\partial T^{(0)}/\partial \nu^+)|_{\Gamma_0}$.

Step 2. (i) If the approximation $T^{(2k)}$ is constructed, solve the mixed well-posed problem

$$LT^{(2k+1)} = 0 \text{ on } \Omega, \qquad T^{(2k+1)} = f \text{ on } \Gamma_1, \qquad \frac{\partial T^{(2k+1)}}{\partial \nu^+} = \mu_k \text{ on } \Gamma_0, \tag{66}$$

to determine $T^{(2k+1)}(\bar{x})$ for $\bar{x} \in \Omega$ and $u_{k+1} = T^{(2k+1)}|_{\Gamma_0}$.
(ii) Having constructed $T^{(2k+1)}$ solve the mixed well-posed problem

$$LT^{(2k+2)} = 0 \text{ on } \Omega, \qquad \frac{\partial T^{(2k+2)}}{\partial \nu^+} = q \text{ on } \Gamma_1, \qquad T^{(2k+2)} = u_{k+1} \text{ on } \Gamma_0 \tag{67}$$

to determine $T^{(2k+2)}(\bar{x})$ for $\bar{x} \in \Omega$ and $\mu_{k+1} = (\partial T^{(2k+2)}/\partial \nu^+)|_{\Gamma_0}$..
Step 3. Repeat step 2 for $k \geq 0$ until a prescribed stopping criterion is satisfied.

The intermediate mixed well-posed problems (66) and (67) are solved using the BEM. A detailed description of the BEM numerical implementation of the iterative algorithm for the Cauchy problem was presented in Mera et al. [9] using constant boundary elements. In addition, a regularising stopping criterion was developed and a relaxation procedure to increase the rate of convergence of the algorithm was proposed. Therefore, only those features necessary to facilitate a concise comparison of the various BEM formulations are presented in this study.

Since in Section 4 it was found that the direct Dirichlet problem is solved more accurately using higher-order interpolation functions for the temperature and the heat flux, it is expected that the same methods will also produce more accurate results for the intermediate mixed well-posed problems that occur when solving the Cauchy problem by the iterative algorithm described in Section 2. It is the purpose of this section to compare the numerical results obtained for the Cauchy problem by using various BEMs to solve these intermediate mixed well-posed problems.

In order to illustrate the performance of the numerical methods proposed we consider the same test example as

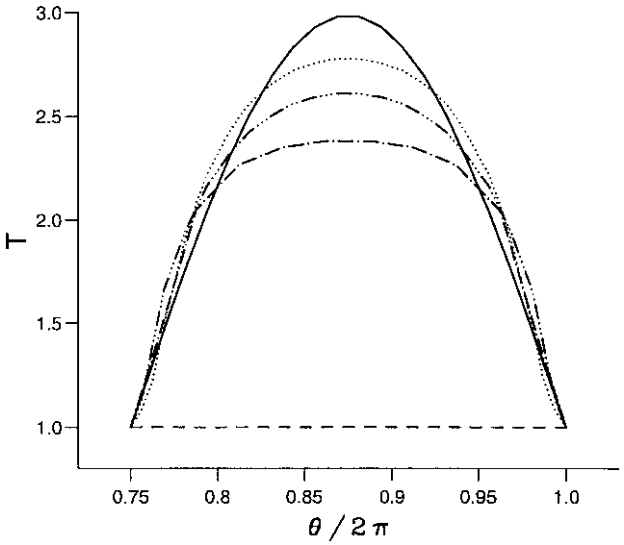

Fig. 3. The numerical solutions for the temperature on the boundary Γ_0 obtained using CBEM (·---), DLBEM (-·-·-) and DQBEM (···) with $N = 40$ boundary elements, in comparison with the analytical solution (—) and the initial guess (- - -), for the Cauchy problem given by Eq. (3).

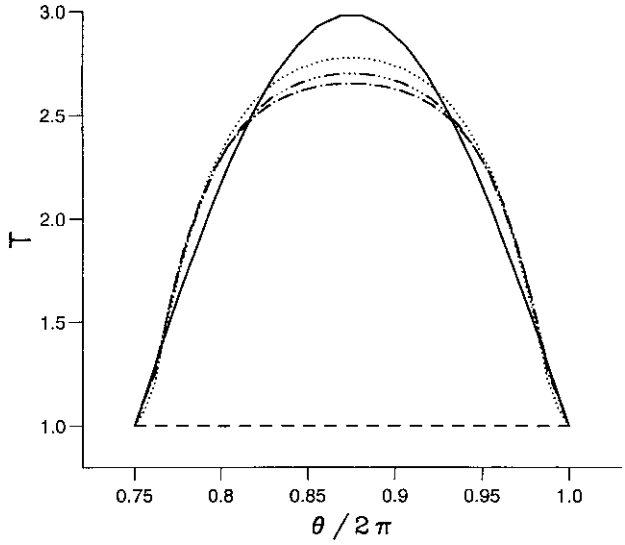

Fig. 4. The numerical solutions for the temperature on the boundary Γ_0 obtained using 120 constant boundary elements (·---), 60 discontinuous linear boundary elements (-·-·-) and 40 discontinuous quadratic boundary elements (···), in comparison with the analytical solution (—) and the initial guess (- - -), for the Cauchy problem given by Eq. (3).

that used in Mera et al. [9], i.e. the thermal conductivity tensor is given by $k_{11} = 1.0$, $k_{12} = 0.5$ and $k_{22} = 1.0$ and the analytical temperature distribution sought as

$$T(x, y) = x^2 - 4xy + y^2 \tag{68}$$

In order to illustrate the typical numerical results for higher-order boundary elements and to compare them with the numerical results obtained by Mera et al. [9] using constant boundary elements, Γ_1 was taken to be $\{\bar{x}|\theta(\bar{x}) \leq 3\pi/2\}$ where θ is the angular polar co-ordinate and an initial guess that ensures the continuity of the temperature at the end-points of the boundary Γ_0 was specified.

Since an arbitrary initial guess may be specified for the temperature on the unspecified part of the boundary Γ_0 it was found that for particular test examples, the intermediate mixed problems (66) and (67) may have discontinuities in the heat flux at the end-points of the boundary Γ_0. Since these points are used as collocation points by the continuous boundary elements (LBEM and QBEM) it was found that these methods may produce inaccurate results for the intermediate mixed problems (66) and (67). For such problems, with discontinuities in the boundary data, discontinuous boundary elements are more appropriate, see Kane [7] and Paris and Canas [10]. Therefore, in this section the Cauchy problem considered is solved using three types of discontinuous boundary elements, namely, constant boundary elements (CBEM), discontinuous linear boundary elements (DLBEM) and discontinuous quadratic boundary elements (DQBEM).

The convergence of the iterative algorithm may be investigated using the convergence error

$$e_T = \|T_{\text{num}} - T_{\text{an}}\|_{L^2(\Gamma_0)} \tag{69}$$

where T_{num} and T_{an} are the numerical and the exact solutions for the temperature on the boundary Γ_0, respectively. For simplicity, the iterative process is stopped at the iteration where the error e_T attains its minimum but similar results are obtained if the regularising stopping criterion proposed by Mera et al. [9] is used to cease the iterations.

Fig. 3 presents the numerical solution for the temperature on the boundary Γ_0 obtained using the CBEM, the DLBEM and the DQBEM for $N = 40$ boundary elements in comparison with the exact solution given by Eq. (68) and the initial guess linear with respect to the angular polar co-ordinate. It can be seen that the numerical solution is substantially improved by using higher-order boundary elements. It should be noted that for the intermediate mixed problems (66) and (67) the solutions obtained using various types of boundary element are in good agreement and are graphically indistinguishable. However, for the problem considered in this section if large numbers of iterations are needed, the errors from the intermediate mixed problems accumulate at every iteration leading to a substantial difference between the solution obtained with constant boundary elements and that obtained with higher-order boundary elements.

Since a system of linear algebraic equations is solved at every iteration and large numbers of iteration are required to achieve convergence, we obtain that whilst the numerical solutions obtained with higher-order boundary elements as presented in Fig. 3 are more accurate, they are also much more expensive in terms of computational time, in comparison with the solution obtained by CBEM. In order to give a more realistic comparison of the methods employed, the Cauchy problem was solved with $N/3$ discontinuous quadratic boundary elements, $N/2$ discontinuous linear

elements and N constant elements, such that for all three methods the system solved is of size $N \times N$, i.e. the numerical solutions obtained are equivalent in terms of the computational time. Fig. 4 presents the numerical solutions obtained for $N = 120$, i.e. 40 quadratic elements, 60 linear elements and 120 constant elements. It can be seen that even if the errors in approximating the boundary by straight lines are increased by reducing the number of boundary elements, the numerical solution obtained for the temperature on the boundary Γ_0 is more accurate if discontinuous linear or discontinuous quadratic boundary elements are used.

Numerous other test examples were investigated and it was found that generally the DQBEM produced more accurate results for the Cauchy problem than the CBEM or the DLBEM. Care must be taken when using linear elements since it was shown in Section 4 that they may produce less accurate results than constant elements, even for simple, direct problems. Therefore, it may be concluded that quadratic boundary elements generally produce more accurate results than linear or constant boundary elements.

However, for particular problems, if the initial guess is far from the exact solution, the numerical solution obtained with CBEM, DLBEM or DQBEM may still be far from the exact solution at the point where the iterative process must be stopped. If this is the case, then relaxation procedures may be used to increase the rate of convergence of the iterative process. Although not illustrated here, it is reported that the variable relaxation factor proposed by Mera et al. [9] for the iterative CBEM was found to produce an increased rate of convergence and substantially improved results also if used in connection with the DLBEM and the DQBEM.

6. Conclusions

In this paper the BEM was employed for solving anisotropic heat conduction problems. Constant elements, continuous and discontinuous linear elements and continuous and discontinuous quadratic elements were used. The performances of these various BEM formulations were compared revealing several features of the BEM.

Analytical formulae for the integrals associated with the BEM for steady state anisotropic heat conduction problems were given since these are not available in the literature and were previously evaluated numerically. The evaluation of these integrals by the analytical formulae presented here requires substantially less computational time than that required by previously employed quadrature formulae. This reduction in terms of computational time is particularly important when solving ill-posed problems by iterative methods, which require a large number of iterations and a direct well-posed problem to be solved at every iteration.

Overall, it can be concluded that all the BEM formulations presented here produce an accurate and convergent numerical solution for anisotropic heat conduction problems. However, if a highly accurate solution is needed, then higher-order boundary elements such as quadratic elements should be used. The discontinuous quadratic elements are also very suitable to deal with corners, discontinuities or singularities.

Appendix A. Analytical formulae for the integrals associated with the BEM for anisotropic heat conduction

As shown in Sections 3.1–3.4, the evaluation of the coefficients of the system of linear algebraic equations obtained by BEM reduces to the evaluation of integrals of the type

$$A(\bar{x}, \bar{x}_1, \bar{x}_2) = \int_\Gamma G_2(\bar{x}, \bar{x}')\, \mathrm{d}\Gamma_{\bar{x}'} \qquad \text{for } \bar{x} = (x, y) \in \bar{\Omega} \tag{A.1}$$

$$B(\bar{x}, \bar{x}_1, \bar{x}_2) = \int_\Gamma \frac{\partial G_2}{\partial \nu^+}(\bar{x}, \bar{x}')\, \mathrm{d}\Gamma_{\bar{x}'} \qquad \text{for } \bar{x} = (x, y) \in \bar{\Omega} \tag{A.2}$$

$$C(\bar{x}, \bar{x}_1, \bar{x}_2) = \int_\Gamma G_2(\bar{x}, \bar{x}')\zeta\, \mathrm{d}\Gamma_{\bar{x}'} \qquad \text{for } \bar{x} = (x, y) \in \bar{\Omega} \tag{A.3}$$

$$D(\bar{x}, \bar{x}_1, \bar{x}_2) = \int_\Gamma \frac{\partial G_2}{\partial \nu^+}(\bar{x}, \bar{x}')\zeta\, \mathrm{d}\Gamma_{\bar{x}'} \qquad \text{for } \bar{x} = (x, y) \in \bar{\Omega} \tag{A.4}$$

$$E(\bar{x}, \bar{x}_1, \bar{x}_2) = \int_\Gamma G_2(\bar{x}, \bar{x}')\zeta^2\, \mathrm{d}\Gamma_{\bar{x}'} \qquad \text{for } \bar{x} = (x, y) \in \bar{\Omega} \tag{A.5}$$

$$F(\bar{x}, \bar{x}_1, \bar{x}_2) = \int_\Gamma \frac{\partial G_2}{\partial \nu^+}(\bar{x}, \bar{x}')\zeta^2\, \mathrm{d}\Gamma_{\bar{x}'} \qquad \text{for } \bar{x} = (x, y) \in \bar{\Omega} \tag{A.6}$$

where

$$G_2(\bar{x}, \bar{x}') = -\frac{|k^{ij}|^{1/2}}{2\pi} \times \ln\left(\sqrt{k^{11}(x - x')^2 + 2k^{12}(x - x')(y - y') + k^{22}(y - y')^2}\right),$$

k_{ij} is the thermal conductivity tensor, k^{ij} is the inverse of the matrix k_{ij}, $|k_{ij}|$ is the determinant of k_{ij} and Γ is the straight line having the endpoints $\bar{x}^1 = (x_1, y_1)$, $\bar{x}^2 = (x_2, y_2)$. These integrals can be computed numerically but in order to obtain an exact value they may be evaluated analytically for every $\bar{x} \in \mathbb{R}^2$ and any straight line Γ. If we denote $c_1 = -(|k^{ij}|^{1/2}/2\pi)h_1$ where h_1 is the length of the segment Γ, $c_2 = (|k^{ij}|^{1/2}/2\pi)$, and we parameterise the line Γ by the function $\gamma : [0, 1] \to \mathbb{R}^2$, $\gamma(\zeta) = (x_1 + \zeta(x_2 - x_1), y_1 +$

$\zeta(y_2 - y_1))$ we obtain

$$A(\bar{x},\bar{x}_1,\bar{x}_2) = c_1 \int_0^1 \ln(\sqrt{a\zeta^2 + b\zeta + c})\, \mathrm{d}\zeta \tag{A.7}$$

$$B(\bar{x},\bar{x}_1,\bar{x}_2) = c_2 \int_0^1 \frac{g}{a\zeta^2 + b\zeta + c}\, \mathrm{d}\zeta \tag{A.8}$$

$$C(\bar{x},\bar{x}_1,\bar{x}_2) = c_1 \int_0^1 \ln(\sqrt{a\zeta^2 + b\zeta + c})\zeta\, \mathrm{d}\zeta \tag{A.9}$$

$$D(\bar{x},\bar{x}_1,\bar{x}_2) = c_2 \int_0^1 \frac{g\zeta}{a\zeta^2 + b\zeta + c}\, \mathrm{d}\zeta \tag{A.10}$$

$$E(\bar{x},\bar{x}_1,\bar{x}_2) = c_1 \int_0^1 \ln(\sqrt{a\zeta^2 + b\zeta + c})\zeta^2\, \mathrm{d}\zeta \tag{A.11}$$

$$F(\bar{x},\bar{x}_1,\bar{x}_2) = c_2 \int_0^1 \frac{g\zeta^2}{a\zeta^2 + b\zeta + c}\, \mathrm{d}\zeta \tag{A.12}$$

where

$$a = k^{11}(x_2 - x_1)^2 + 2k^{12}(x_2 - x_1)(y_2 - y_1) + k^{22}(y_2 - y_1)^2$$

$$b = -2k^{11}(x_2 - x_1)(x - x_1) - 2k^{22}(y_2 - y_1)(y - y_1) - 2k^{12}(x - x_1)(y_2 - y_1) - 2k^{12}(y - y_1)(x_2 - x_1)$$

$$c = k^{11}(x - x_1)^2 + 2k^{12}(x - x_1)(y - y_1) + k^{22}(y - y_1)^2$$

$$g = (y_2 - y_1)(x - x_1) - (x_2 - x_1)(y - y_1)$$

$$I_1(a,b,c) = \int_0^1 \frac{\mathrm{d}\zeta}{a\zeta^2 + b\zeta + c} = \begin{cases} \dfrac{4a}{b(2a+b)} & \text{if } b^2 - 4ac = 0 \\ \dfrac{1}{\sqrt{b^2 - 4ac}} \ln\left| \dfrac{2a + b - \sqrt{b^2 - 4ac}}{2a + b - \sqrt{b^2 + 4ac}} \dfrac{b + \sqrt{b^2 - 4ac}}{b - \sqrt{b^2 - 4ac}} \right| & \text{if } b^2 - 4ac > 0 \\ \dfrac{2}{\sqrt{4ac - b^2}} \left(\tan^{-1}\left(\dfrac{2a + b}{\sqrt{4ac - b^2}} \right) - \tan^{-1}\left(\dfrac{b}{\sqrt{4ac - b^2}} \right) \right) & \text{if } b^2 - 4ac < 0 \end{cases}$$

A.1. The collocation point does not belong to the boundary element

If the collocation point $\bar{x}$ does not belong to the straight line Γ, a and c may not be zero,

$$\Delta = 4(k^{12})^2 - 4k^{11}k^{22} = \frac{4}{k_{12}^2 - k_{11}k_{22}} < 0,$$

and integrating by parts we obtain

$$\frac{A(\bar{x},\bar{x}_1,\bar{x}_2)}{c_1} = \ln\sqrt{a + b + c} - 1 + \frac{b}{4a} \ln\left(\frac{a + b + c}{c} \right) + \frac{4ac - b^2}{4a} I_1(a,b,c) \tag{A.13}$$

$$B(\bar{x},\bar{x}_1,\bar{x}_2) = gc_2 I_1(a,b,c) \tag{A.14}$$

$$\frac{C(\bar{x},\bar{x}_1,\bar{x}_2)}{c_1} = \frac{1}{2} \ln\sqrt{a + b + c} - \frac{1}{4} + \frac{1}{4} I_2(b, 2c, 0, a, b, c) \tag{A.15}$$

$$D(\bar{x},\bar{x}_1,\bar{x}_2) = c_2 I_2(0, g, 0, a, b, c) \tag{A.16}$$

$$\frac{E(\bar{x},\bar{x}_1,\bar{x}_2)}{c_1} = \frac{1}{3} \ln\sqrt{a + b + c} - \frac{1}{9} + \frac{b}{12a} + \frac{b}{6a} I_2\left(\frac{2ac}{b} - b, -c, 0, a, b, c \right) \tag{A.17}$$

$$F(\bar{x},\bar{x}_1,\bar{x}_2) = c_2 I_2(g, 0, 0, a, b, c) \tag{A.18}$$

where

$$I_2(d,f,g,a,b,c) = \int_0^1 \frac{d\zeta^2 + f\zeta + g}{a\zeta^2 + b\zeta + c}\, \mathrm{d}\zeta = \frac{d}{a} + \frac{1}{2a}\left(f - \frac{bd}{a} \right) \ln\frac{a + b + c}{c} + \left[-\frac{b}{2a}\left(f - \frac{bd}{a} \right) + g - \frac{cd}{a} \right] I_1(a,b,c)$$

and

A.2. The collocation point belongs to the boundary element

In the BEM formulations considered, if the collocation point $\bar{x}$ belongs to the boundary element Γ then the integrals (A.1)–(A.6) becomes singular. First, we consider the case when the collocation point $\bar{x}$ is an internal point of the segment Γ. This kind of singular integral appears in CBEM, QBEM, DLBEM and DQBEM. If the integrals (A.1)–(A.6) are evaluated as improper integrals it can be seen that the same formulae obtained for the non-singular

case, namely, Eqs. (A.13)–(A.18), may be used to evaluate the singular integrals obtained by taking the collocation point $\bar{x}$ as an internal point of the segment Γ.

A second type of singular integral arises in the LBEM and QBEM when the boundary integral equation is applied at the interval points $\bar{x}_j, j = \overline{1,N}$. Thus, the collocation point $\bar{x}$ is one of the end-points of the interval Γ. If this is the case the integrals (A.1)–(A.6) are evaluated as improper integrals or in the sense of their Cauchy principal value and the following formulae are obtained

$$A(\bar{x}_1,\bar{x}_1,\bar{x}_2) = c_1 \int_0^1 \ln(\sqrt{a\zeta^2})\,\mathrm{d}\zeta = c_1(\ln\sqrt{a} - 1) \tag{A.19}$$

$$A(\bar{x}_2,\bar{x}_1,\bar{x}_2) = c_1 \int_0^1 \ln(\sqrt{a(\zeta-1)^2})\,\mathrm{d}\zeta = c_1(\ln\sqrt{a} - 1) \tag{A.20}$$

$$C(\bar{x}_1,\bar{x}_1,\bar{x}_2) = c_1 \int_0^1 \ln(\sqrt{a\zeta^2})\zeta\,\mathrm{d}\zeta = \frac{c_1}{2}\left(\ln\sqrt{a} - \frac{1}{2}\right) \tag{A.21}$$

$$C(\bar{x}_2,\bar{x}_1,\bar{x}_2) = c_1 \int_0^1 \ln(\sqrt{a(\zeta-1)^2})\zeta\,\mathrm{d}\zeta = \frac{c_1}{2}\left(\ln\sqrt{a} - \frac{3}{2}\right) \tag{A.22}$$

$$E(\bar{x}_1,\bar{x}_1,\bar{x}_2) = c_1 \int_0^1 \ln(\sqrt{a\zeta^2})\zeta^2\,\mathrm{d}\zeta = \frac{c_1}{3}\left(\ln\sqrt{a} - \frac{1}{3}\right) \tag{A.23}$$

$$E(\bar{x}_2,\bar{x}_1,\bar{x}_2) = c_1 \int_0^1 \ln(\sqrt{a(\zeta-1)^2})\zeta^2\,\mathrm{d}\zeta = \frac{c_1}{3}\left(\ln\sqrt{a} - \frac{11}{6}\right) \tag{A.24}$$

$$B(\bar{x}_1,\bar{x}_1,\bar{x}_2) = B(\bar{x}_2,\bar{x}_1,\bar{x}_2) = 0 \tag{A.25}$$

$$D(\bar{x}_1,\bar{x}_1,\bar{x}_2) = D(\bar{x}_2,\bar{x}_1,\bar{x}_2) = 0 \tag{A.26}$$

$$F(\bar{x}_1,\bar{x}_1,\bar{x}_2) = F(\bar{x}_2,\bar{x}_1,\bar{x}_2) = 0 \tag{A.27}$$

References

[1] Brebbia CA. The boundary element method for engineers. London: Pentech Press, 1978.

[2] Brebbia CA, Telles JCF, Wrobel LC. Boundary element techniques: theory and application in engineering. Berlin: Springer, 1984.

[3] Chang YP, Kang CS, Chen DJ. The use of fundamental Green's functions for the solution of heat conduction in anisotropic media. Int J Heat Mass Transfer 1973;16:1905–18.

[4] Hadamard J. Lectures on Cauchy problem in linear partial differential equations. New Heavens: Yale University Press, 1923.

[5] Ingham DB, Heggs PJ, Manzoor M. The numerical solution of plane potential problems by improved boundary integral equation methods. J Comput Phys 1981;42:77–98.

[6] Jawson MA, Symm GT. Integral equation methods in potential theory and elastostatics. London: Academic Press, 1977.

[7] Kane JH. Boundary element analysis in engineering continuum mechanics. Englewood Cliffs, NJ: Prentice Hall, 1994.

[8] Kozlov VA, Maz'ya VG, Fomin DV. An iterative method for solving the Cauchy problem for elliptic equation. Comput Math Math Phys 1991;31:45–52.

[9] Mera NS, Elliott L, Ingham DB, Lesnic D. The effect of a variable relaxation factor on the rate of convergence in the Cauchy problem. In: Aliabadi MH, editor. Boundary element technique. London: Queen Mary and Westfield College, University of London, 1999. p. 357–66.

[10] Paris F, Canas J. Boundary element method: fundamentals and applications. Oxford: Oxford University Press, 1997.

[11] Patterson C, Sheikh MA. Discontinuous boundary elements for heat equation. In: Lewis RW, et al., editors. Numerical methods for thermal problems. Southampton: Pineridge Press, 1981. p. 25–35.

[12] Subia SR, Ingber MS, Mitra AK. A comparison of the semidiscontinuous element and multiple node with auxiliary boundary collocation approaches for the boundary element method. Eng Anal Bound Elem 1995;15:19–27.